J. Membrane Biol. 73, 193–202 (1983)

The Journal of
Membrane Biology


# Membrane Conductance of *Chara* Measured in the Acid and Basic Zones

J.R. Smith and N.A. Walker
Biophysics Laboratory, School of Biological Sciences, University of Sydney A12, New South Wales 2006, Australia

**Summary.** A sinusoidal AC current (usually at 1 Hz) was injected into either the acid or basic zone present in illuminated internodal cells of *Chara*. The "cable" properties of the cell were then studied by two techniques. The first involved measuring the dependence of the transverse AC membrane current (measured in the external medium) upon the distance away from the point of current injection. The second measured the AC membrane voltage at two different positions along the cell. It was found that AC current injected into an illuminated basic region left the cell close to the point of current injection, the effective cable length $\lambda_B$ being typically 3 to 5 mm. For AC current injected into an illuminated acid zone however, the cable length $\lambda_A$ was significantly longer ($\approx$10 to 15 mm). From considerations of the properties of electrically inhomogeneous cables it was possible to estimate the individual area-specific conductances of the acid and basic zones. In strong illumination the conductance of the acid zones was typically 0.8 to 1.0 S/m$^2$, whereas that of the basic zones was much higher ($\approx$5 to 8 S/m$^2$). Upon removal of illumination the conductance of each zone was found to slowly decrease, and after several hours the membrane conductance was relatively homogeneous over the cell surface. The large degree of longitudinal spatial inhomogeneity in the membrane conductance of illuminated *Chara* cells has important consequences for the interpretation of experimental results, and can produce large errors in the estimated membrane area-specific conductance if these inhomogeneities are not explicitly recognized and accounted for. An examination of the literature suggests that previous measurements utilizing point current injection might indeed have systematically underestimated the area-specific membrane conductance of *Chara*.

**Key Words** conductance · *Chara* · banding · proton pump · pH · membrane

## Introduction

It is known that cells of *Chara* and *Nitella* can develop spatially distinct acid and basic regions in the external medium adjacent to the cell upon exposure to light (e.g. Spear, Barr & Barr, 1969; Lucas & Smith, 1973). Associated with the maintenance of these large pH gradients along the cell surface are large electric currents (Walker & Smith, 1977) which produce associated small variations in the electric potential difference (PD) measured along the surface of the cell.

Recent experiments with *Chara* cells suspended in air using a water-film electrode technique [1] have given values for the "open-circuit" PD between the acid and basic regions, and have shown that the membrane PD (plasmalemma and tonoplast in series) in the acid zones [2] is then hyperpolarized by $\sim$50 to 60 mV with respect to that in the basic zones. This suggests that the electrical properties of the acid and basic zones can be quite different. Indeed while suspended in air, the area-specific conductance of the basic zones can be typically 6 times greater than that of the acid zones (Chilcott, Coster, Ogata & Smith, 1981 [3]). Additionally, the frequency dependence of the membrane capacitance and conductance in the acid and basic zones were found to differ. Thus the electrical parameters of *Chara* cells suspended in air are spatially inhomogeneous.

Bisson and Walker (1980, 1981) showed that the membrane conductance can increase markedly ($\sim$5 times) when the pH of the solution bathing a *Chara* cell approaches the value normally found in a basic region. This further suggests that the conductance of the basic zones may well be significantly higher than that of the acid zones when cells are bathed in an aqueous medium. Indeed it has been suggested (e.g. Walker, 1980; Bisson

[1] Ogata, K., Chilcott, T.C., Coster, H.G.L. Spatial variation of the electrical properties of *Chara*: I. Electrical potentials and membrane conductance. *Aust. J. Biol. Sci. (Submitted)*.

[2] In this paper acid or basic zones will refer to the regions of the cell membrane which, upon illumination, would produce, respectively, acid or basic regions in the external medium (*see* Walker & Smith, 1977).

[3] Chilcott, T.C., Coster, H.G.L., Ogata, K., Smith, J.R. Spatial variation of the electrical properties of *Chara*: II. Membrane capacitance and conductance as a function of frequency. *Aust. J. Plant Physiol. (Submitted)*.

& Walker, 1982) that the plasmalemma could be in distinctly different electrochemical states in the acid and basic zones. Verification of whether the conductance of illuminated *Chara* cells is indeed spatially inhomogeneous under normal experimental conditions, i.e. when bathed in an aqueous solution rather than in air, is important because of its consequences in the interpretation of electrical measurements (*see* Smith, 1983). Additionally, such measurements could help to elucidate the mechanisms involved in the production of pH banding.

In an accompanying paper (Smith, 1983) it was demonstrated how the area-specific conductance of an individual membrane region within a spatially inhomogeneous cylindrical cell could be evaluated from knowledge of the characteristic (or cable) length for the decay of either the transverse electric current or the resultant membrane PD adjacent to the point of current injection. Using this approach we have estimated the separate conductances of the basic and acid zones in *Chara* during pH banding and while cells are bathed in an artifical pond water (APW). Additionally, the effect of the removal of illumination upon these conductances has been studied.

## Materials and Methods

Long (~40 mm) straight internodal cells of *Chara australis* (R.Br.) with diameters 0.6 to 0.9 mm were used. Cells with visible calcification were generally chosen to facilitate the desired positioning of the acid and basic zones within the perspex cell holder which was divided into three electrically isolated sections via silicon grease packed tightly around the cell surface when blotted dry. Artificial pond water (APW −0.1 mM KCl, 1.0 mM NaCl, 1.0 mM $CaCl_2$, pH ≈5.5) was then added to each section. Location of the acid and basic regions was verified by the addition of a small amount of pH indicator (phenol red) to the bathing solution. Measurements were performed at room temperature (22 ± 2 °C) with illumination (~100 μE·$m^{-2}$ $sec^{-1}$) provided by a microscope light when desired. It was found that the membrane conductance could take several hours to reach its final value in the dark. Thus cells for dark measurements were often preconditioned by leaving them overnight in the dark. The bathing solutions were changed periodically, but were stagnant during measurements. The cell length in the measuring chamber was always sufficient to ensure that acid and basic zones were both always present and that pH banding (as revealed by phenol red) was present upon illumination.

Unless otherwise indicated the membrane conductance was measured at 1 Hz, a frequency sufficiently low to adequately reflect the DC membrane conductance (e.g. Coster & Smith, 1977). The sinusoidal AC signal at the desired frequency was generated by a computer (Cromemco Z2-D) and passed between a Ag/AgCl electrode located in an outer region and another such electrode located immediately adjacent to the edge of the measuring chamber and extending across its width (*see* Figs. 1 and 2). Thus AC current was effectively injected into the cell section under study at $x=0$. The appropiate zone under investigation was located at the edge of the measuring chamber near the latter Ag/AgCl electrode (i.e. at $x=0$). The total AC current $I_T$ flowing through the membrane in the measuring chamber was derived from the AC PD. $V_R$ developed across a series resistor $R$. This approach assumes that all the AC current will flow between sections of the cell holder via the vacuole. Some current, however, will flow via the cytoplasm and cell wall. Calculations suggest that the error produced by the neglect of these pathways will be at most a few percent.

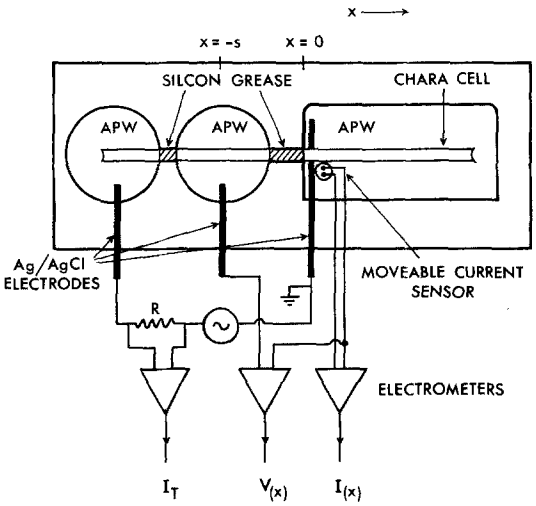


**Fig. 1.** Schematic diagram of the experimental apparatus in which the spatial decay of the transverse membrane current as measured by external electrodes was used to determine the effective cable length

The sinusoidal responses of $I_T$, $V(x)$ and $I(x)$, where $V(x)$ and $I(x)$ are the membrane PD and transverse current, respectively, at position $x$, were measured by the computer (256 samples for each parameter per cycle) via an analog to digital converter (8 bit). Their amplitudes and relative phases were extracted as described previously (Bell, Coster & Smith, 1975) by fitting to a general sinusoidal function using the method of least-squares. From the index of correlation for each fit, the magnitude of any noise and nonlinearity present could be monitored. Correlation indices were typically ≈0.998, and any data with an index less than 0.98 was usually discarded.

The measured admittance $Y^*$ at the point of current injection was then calculated from

$$Y^* = I_T/V(0) = V_R/(R\,V(0)) \quad (1)$$

where $V(0)$ is the AC membrane PD at $x=0$. The measured conductance $G^*$ is then simply the real part of the complex admittance $Y^*$. The overall precision of these conductance measurements was typically 0.5 to 1%. The impedance $Z$ is the reciprocal of the admittance (i.e. $Z=1/Y$).

### *Measurements of Decay of Transverse AC Current*

A schematic diagram of the apparatus used is given in Fig. 1. The transverse AC electric current $I(x)$ flowing through the plasmalemma was monitored from the AC PD. $V_E(x)$ developed between a pair of moveable Ag/AgCl electrodes located immediately adjacent and perpendicular to the cell surface. This pair of Ag wires (diam ~300 μm) were Teflon®-coated (diam ~350 μm) with a typical center-center spacing of 0.5 mm and were constrained inside a glass capillary tube. They could be accurately moved longitudinally and adjacent to the cell surface by means of a micromanipulator driven by a stepping motor under control of the computer, and could be reproducibly located in ~80-μm steps. $I(x)$ is related to $V_E(x)$ via the relationship

$$I(x) = V_E(x)/R_E \quad (2)$$

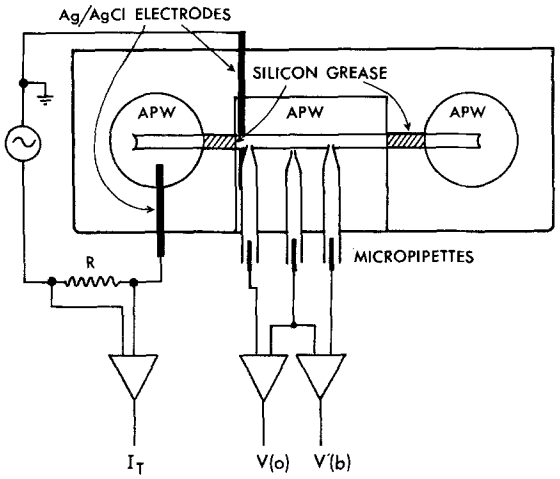


**Fig. 2.** Schematic diagram of the experimental apparatus in which internal microelectrodes were used to determine the decay with distance of the AC membrane PD and hence determine the cable length. For clarity the microelectrode tips have been illustrated with a greater separation than was actually used in the experiments. The tip of the microelectrode in the external solution was located immediately adjacent to the cell surface at $x=0$

where $R_E$ is the resistance of the external electrolyte between the electrode tips and was assumed to be independent of position over the cell surface. The performance of these electrode pairs could be checked before use by their placement in a chamber of APW containing two parallel silver wires between which a known AC current was passed. Because only relative changes in the magnitudes of the currents were used in the analysis, no attempt was made to provide an absolute calibration for each electrode pair. Experiments conducted with a dummy cell (a Teflon-coated Ag wire with the coating removed for $\approx 1$ mm at $x=0$) suggested that the spatial resolution would be approximately 0.1 to 0.25 mm. In experiments the cable length $\lambda$ was always found to be larger than the cell diameter. This implies that the current distribution through the membrane should be essentially radially symmetric. Thus it might be expected that the presence of the current-sensing electrode adjacent to one point on the cell surface should not significantly affect the distribution of the current flow in the external medium.

The AC PD $V(0)$ produced across the membrane at $x=0$ as a consequence of the applied AC current was determined from measurements of the AC PD $V^*(0)$ developed between two Ag/AgCl electrodes; one located in the measuring chamber adjacent to the cell surface at $x=0$ and the other located in a separate section at $x=-s$. Only an extremely small AC current flowed through the membrane via the electrometer in this latter section, and hence a negligible AC PD was developed across the membrane, i.e. the AC potential in this section effectively approximated that of the vacuole.

An AC PD $V_v$ will then be present in the vacuole between these two sections as a consequence of the current $I_T$ and is related to the longitudinal resistance per unit length of the vacuole ($r_i$) via the relation

$$V_v = r_i s I_T. \tag{3}$$

Then $V(0)$ can be calculated from

$$V(0) = V^*(0) - V_v. \tag{4}$$

The experimental procedure involved first locating the moveable electrode pair immediately adjacent to the point of current injection (i.e. $x=0$). The tips of these electrodes were adjusted into the mid-plane of the cell and placed as close as possible to the cell surface. The measured conductance $G^*$ (i.e. the real part of $I_T/V(0)$) was then monitored until it became steady. The computer then measured $I(x)$ at the desired coordinates along the cell surface (usually at 50 to 100 points) by using the stepping motor. This procedure usually took 3 to 5 min. To minimize the effects of drift in the membrane characteristics, the value of $I(x)$ measured at each point was normalized with respect to the value of $I_T$ measured simultaneously. The characteristic or cable length $\lambda$ was then calculated; either from the slope of a logarithmic plot of the modulus of $I(x)$ against $x$ (e.g. *see* Fig. 3) or from the distance at which $I(x) = I(0)/e$.

The value of $r_i$ for the cells used was determined from the longitudinal conductance measured at high frequencies (typically 1 to 25 kHz) using external electrodes in a separate series of experiments.

## *Measurements of the Decay of the AC Membrane PD*

The AC membrane PD was measured at two points ($x=0$ and $x=b$) via micropipettes (filled with 3 M KCl) inserted into the vacuole (*see* Fig. 2). The cable length $\lambda$ was then calculated from the relationship

$$V(b)/V(0) = \cosh((l-b)/\lambda)/\cosh(l/\lambda). \tag{5}$$

The separation between the tips of the two microelectrodes was generally kept small for the basic zones to ensure that the cable length measured reflected that at the point of current injection. The calcification of the basic regions, however, often made insertion into the region itself very difficult. It was also found to be impossible to physically locate four microelectrodes into the very small space around the cell and consequently the vacuolar PD $V'(b)$ was usually measured with respect to the external solution at $x=0$. The AC membrane PD $V(b)$ could be calculated from

$$V(b) = ((1+\gamma)V'(b) - V(0))/\gamma \tag{6}$$

where $\gamma$ is the ratio of the longitudinal PD developed in the external solution to that of the vacuole (i.e. $r_o/r_i$).

## *Calculation of Membrane Area-Specific Conductance*

The area-specific conductance of the membrane at the point of current injection was calculated using the following techniques (for full theoretical details *see* Smith, 1983). For the acid zones the membrane was treated as homogeneous and conventional cable theory applied (e.g. Williams, Johnston & Dainty, 1964). This is a reasonable approximation because theoretical calculations show that the presence of distant, more conductive basic zones should not drastically affect the measured conductance (possible error $\sim 10$ to 20%). The conductance of the acid zones was thus calculated from the measured conductance $G^*$ and cable length $\lambda_A$ via the following equation:

$$G_A = G^*/\pi d\lambda_A \tanh(l/\lambda_A) \tag{7}$$

where $d$ and $l$ are, respectively, the diameter and length of the cell section under study.

Cells with basic zones with a width $b$ either approaching that of the entire cell section, or large in comparison with the measured $\lambda_B$, could be treated as homogeneous without much error. Usually for current injection into a basic zone, however, an iterative procedure employing the theory of an inhomogeneous cable was necessary. The model used is relatively insensi-

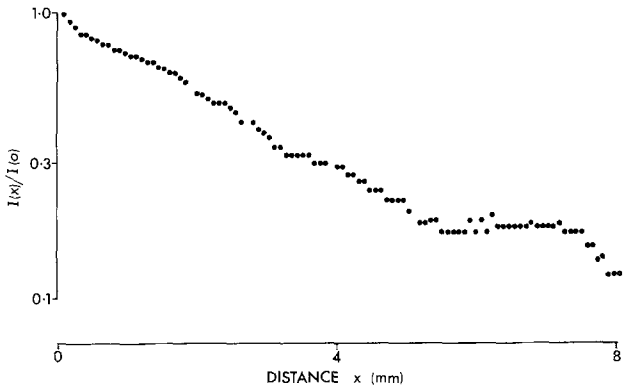


**Fig. 3.** Transverse current $I(x)$ measured in the external solution as a function of distance away from the point of current injection (at $x=0$) into an illuminated basic zone. The data has been normalized with respect to $I(0)$ and plotted on a logarithmic scale. Phenol red indicator suggested that the basic region extended from $x=0$ to $x \approx 5$ mm. From the slope $\lambda_B$ was calculated as 3 mm

tive to the properties of the acid zones and so the average values of $\lambda_A$ and $G_A$ from experiments on different cells were used. The width of the basic zone was estimated by using phenol red. An initial guess for $G_B$ was then made, and the expected value of the measured conductance $G^*$ evaluated using the measured value of $\lambda_B$. $G_B$ was then varied and the procedure repeated until the calculated value of $G^*$ coincided with that measured experimentally.

## Results

### *Measurement of the Transverse AC Current*

Figure 3 shows the transverse AC current $I(x)$ through the membrane (as measured in the external solution) plotted on a logarithmic scale as a function of distance away from the point of current injection (at $x=0$) into an illuminated basic zone. It is evident that for this cell the decay appeared exponential for the initial 5 to 6 mm. $\lambda_B$ was then

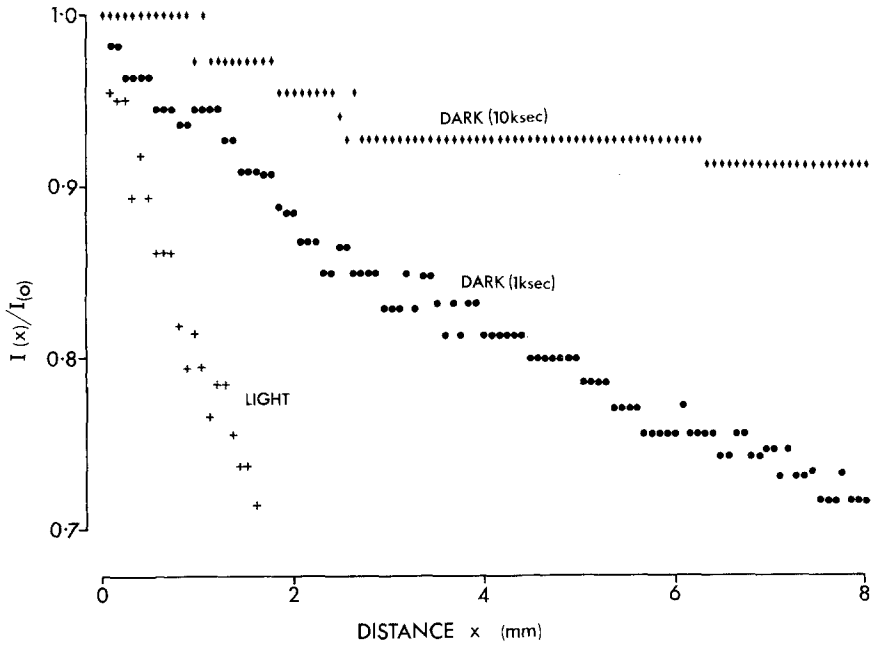


**Fig. 4.** Transverse membrane current $I(x)$ measured in the external solution as a function of distance away from the point of current injection (at $x=0$) into a basic zone of width $\approx 2$ mm. The symbols (+) refer to strong illumination. Once the illumination was removed, the cable length was seen to increase. The symbols (•) and (♦) indicate the results obtained 1 ksec and 10 ksec, respectively, after removal of illumination. The "quantized" nature of the results is a consequence of the analog to digital conversion process. The cable lengths were estimated as 4.7, 17 and 33 mm, respectively

**Table.** Measured electrical parameters of *Chara*

| Technique | Illumination | Acid | | Basic | |
|---|---|---|---|---|---|
| | | $\lambda_A$ (mm) | $G_A$ (S/m$^2$) | $\lambda_B$ (mm) | $G_B$ (S/m$^2$) |
| $I(x)$ | light | – | 0.8 ±0.1 (12) | 3.5±0.7 (11) | 6.2 ±1.6 (11) |
| $I(x)$ | dark | – | 0.21±0.01 (5) | – | 0.34±0.06 (7) |
| $V(x)$ | light | 13.2±1.1 (7) | 1.0 ±0.1 (7) | 4.4±1.1 (6) | 5.6 ±0.5 (7) |

Data presented as mean ± standard error (number of cells).

calculated from the slope. In several cells the decay was not a simple exponential (*see* Discussion) and in these cases $\lambda_B$ was taken as the distance where $I(x)$ had decayed to a value of $1/e$ of $I(0)$. Thus $\lambda_B$ was found to be in the range 0.8 to 7.0 mm for the 11 cells studied.

For current injection into illuminated acid zones, however, the rate of decay of the transverse current with distance away from the point of current injection was far less. Indeed it was very difficult to determine $\lambda_A$ accurately. This was primarily because the maximum current density close to $x=0$ was much lower for acid rather than basic regions because the current flowed through a larger membrane area. The density was typically smaller by a factor of 3 to 10 if the AC membrane PD was to be kept below 10 mV rms. It was also found to be difficult to reliably maintain the relative position of the current electrode with respect to the cell surface over the longer distances involved.

Figure 4 shows the measured decay of the transverse AC membrane current $I(x)$ as a function of distance away from the point of current injection into a basic zone on a different cell than shown in Fig. 3. Upon the removal of illumination the spatial rate of decay of transverse current was seen to progressively decrease, i.e. the cable length increased. This provides evidence that the measured spatial decay of injected current was really related to the membrane electrical properties, rather than its origin being in some artifact of the experimental apparatus or technique.

The Table gives the area-specific membrane conductance for the acid and basic zones calculated as described in Materials and Methods. In the light the basic zones ($6.2\pm1.6$ S/m$^2$) were found to be much more conductive than the acid zones ($0.8\pm0.1$ S/m$^2$). This difference was found to be greatly reduced after long periods (at least 3 hr) in the dark.

It would be expected that the cable length $\lambda$ should be related to the membrane impedance times unit length ($z_m$) via the following relation

$$\lambda=(z_m/(r_o+r_i))^{\frac{1}{2}}. \tag{8}$$

Thus a plot of measured $\lambda$ against $z^{\frac{1}{2}}$ should yield a linear relationship. Figure 5 shows the results of experiments on the basic zone of 11 cells plotted in this fashion. Although there is considerable variation from cell to cell, an overall linear dependence is still evident. From the slope of the line of best fit, $(r_o+r_i)$ was calculated as 7 MΩ/m. Measurements at very high frequencies suggest that $r_i\approx$

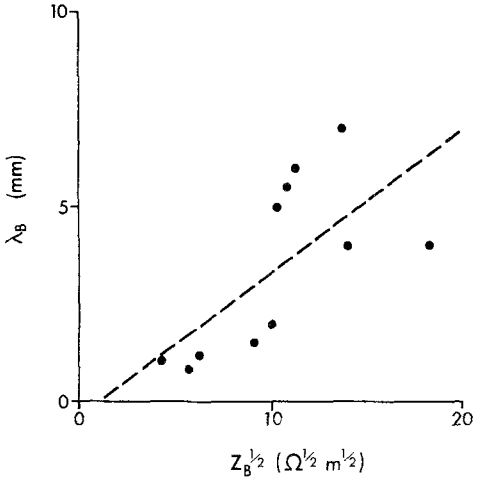


**Fig. 5.** Relationship between the measured cable length $\lambda_B$ and the square root of the measured membrane impedance times unit length $(z_B)^{\frac{1}{2}}$ for current injection into illuminated basic zones. Each point refers to a different one of the 11 cells studied via measurements of the spatial decay of $I(x)$. The dashed line indicates the line of best fit

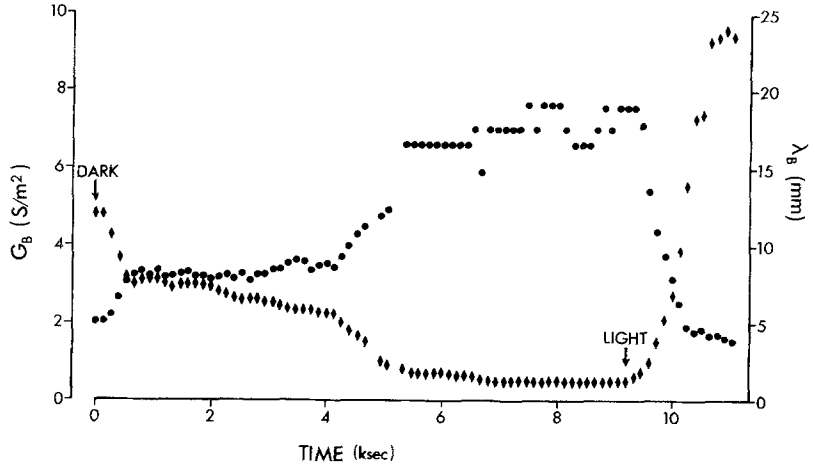


**Fig. 6.** Time dependence of the measured area-specific conductance $G_B$ (♦) and cable length $\lambda_B$ (●) measured from the spatial decay of $V(x)$ for current injection into a basic zone of width 7 mm. The illumination was removed at time 0 and restored 9.2 ksec later

1.5 MΩ/m. The longitudinal cross-sectional area of the chamber used was 16 mm$^2$, and so $r_o$ for the APW used should be ≈2.35 mΩ/m.

### *Measurement of the Spatial Decay of Membrane PD*

On 14 cells the cable length and area-specific membrane conductance were calculated from measurements of the spatial decay of the membrane PD $V(x)$ (*see* Materials and Methods). The results for illuminated cells are summarized in the Table. It is again apparent that the conductance of illuminated basic zones is much higher than acid zones. Upon the removal of illumination, the measured cable length was again found to increase in conjunction with a decrease in the area-specific conductance. Figure 6 shows a representative example for current injection into a basic zone.

As a test of whether this technique appears to be valid, plots of the measured $\lambda$ against $z^{\frac{1}{2}}$ are now presented. Figure 7 shows such a plot for current injection into the acid zone for a single cell. The different values of $z_A$ were obtained in this case by varying the AC frequency $f$ at which the impedance was measured. If the area-specific conductance and capacitance of the membrane are C and $G$, respectively, and $\omega$ is the angular frequency ($\omega = 2\pi f$), then from Eq. (21) of Smith (1983)

$$z = 1/\pi d(G^2 + \omega^2 C^2)^{\frac{1}{2}}. \quad (9)$$

Thus as $\omega$ is increased the measured $z$ will decrease..

Figure 8 shows the results of plotting $\lambda_B$ against $(z_B)^{\frac{1}{2}}$ for current injection into the basic zone of a single cell (the same cell as Fig. 6). Figure 8*a* shows the relationship at an AC frequency of 1 Hz during the removal of illumination and its subsequent restoration. It is apparent that an effectively linear relationship existed throughout the 10 ksec duration of the experiment and over a 20-fold variation in conductance. Figure 8*b* shows the results whereby the AC frequency was varied at three separate times during this experiment. There are some slight differences between Figs. 8*a* and 8*b*, but they

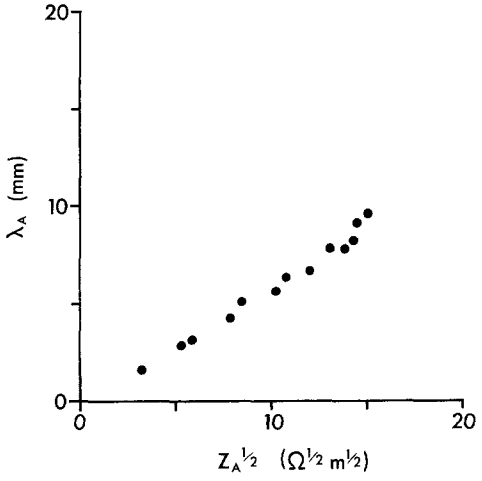


**Fig. 7.** Relationship between the measured cable length $\lambda_A$ and the square root of the membrane impedance times unit length $(z_A)^{\frac{1}{2}}$ for current injection into an illuminated acid zone. Each point is for the same cell and was calculated from the spatial decay of $V(x)$ at a different frequency of the applied AC current (range 0.25 to 128 Hz)

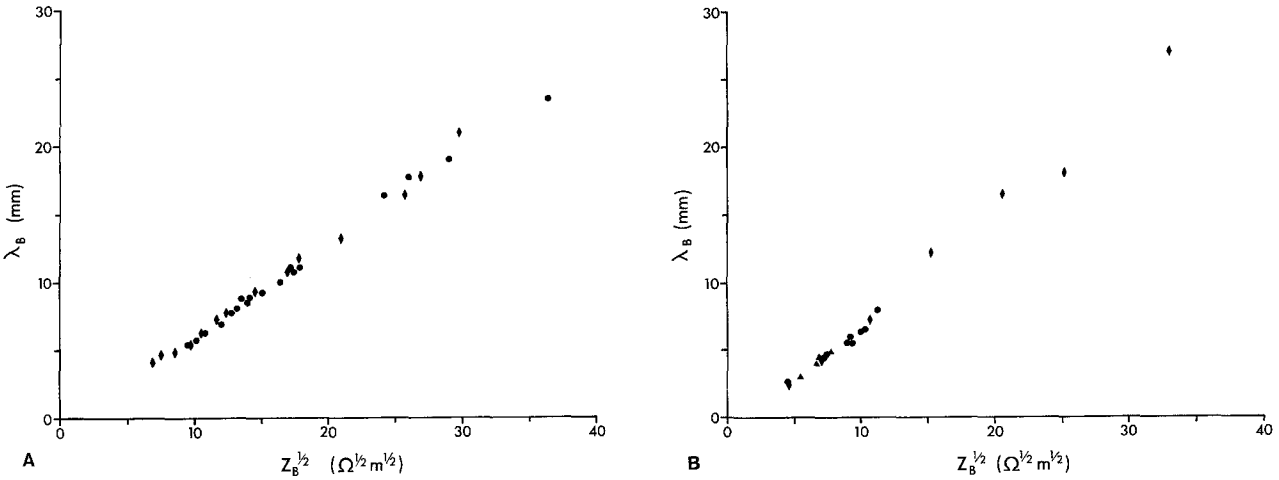


**Fig. 8.** Relationship between the measured cable length $\lambda_B$ and the square root of the membrane impedance times unit length $(z_B)^{\frac{1}{2}}$ for current injection into a basic zone. The data are from the same cell as Fig. 6, and were measured from the spatial decay of $V(x)$. The points shown in Fig. 8*a* were measured at 1 Hz for different times after the removal of illumination (●) and its subsequent restoration (♦) (*see* Fig. 6). The points shown in Fig. 8*b* were obtained at different AC frequencies at three different times. The symbols ●, ♦ and ▲ refer to measurements made, respectively, during initial illumination, after 9 ksec of darkness and after the restoration of illumination

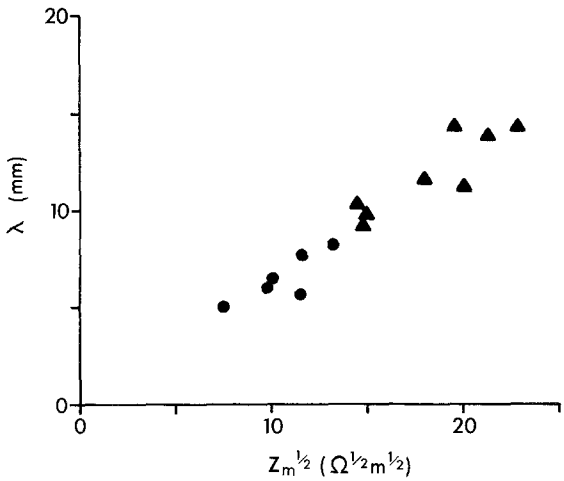


**Fig. 9.** Relationship between the measured cable length $\lambda$ and the square root of the membrane impedance times unit length $(z_m)^{\frac{1}{2}}$ measured by the spatial decay of $V(x)$ at 1 Hz. Each point refers to a different cell. The symbols ● and ▲ refer, respectively, to basic or acid zones

show that the predicted relationship between $\lambda$ and $z^{\frac{1}{2}}$ holds over a very wide range of conditions.

Figure 9 shows a plot of $\lambda$ against $z^{\frac{1}{2}}$ measured at 1 Hz for the 14 cells studied for current injection into illuminated acid and basic zones. It is evident that the relationship is similar for both the acid and basic zones. From the slope of graphs such as Fig. 7 plotted for each of the cells studied, $(r_o + r_i)$ was calculated as $2.45 \pm 0.13$ (14) MΩ/m. The longitudinal cross-sectional area of the chamber used was 40 mm$^2$ and so for the APW used $r_o$ would be expected to be $\approx 0.93$ MΩ/m. The value of $(r_o + r_i)$ calculated from the slope is thus close to that expected from the geometry of the chamber, i.e. $1.5 + 0.93 = 2.43$ MΩ/m.

The measured values for $\lambda_A$ were found to be in the approximate range 10–15 mm (*see* Fig. 9). Similar values would be expected from measurements where spatial inhomogeneity is neglected. Previous measurements on *Nitella flexilis* (Volkov & Platonova, 1970) found $\lambda \sim 13$ mm, whereas measurements on *N. translucens* (Williams et al., 1964; Bradley & Williams, 1967; Hogg, Williams & Johnston, 1969) found $\lambda = 25$–$30$ mm. The difference in the latter results presumably reflects their lower values of both $G$ and $(r_o + r_i)$.

## Discussion

The most striking feature of the results presented here is the enhanced conductance (5 to 8 times greater) of the illuminated basic zones in comparison with the acid zones. The magnitude of the difference is comparable with that reported previously (Bisson & Walker, 1980, 1981) when the pH of the bathing solution approached that expected to be present in a basic region during pH banding (~ pH 10 to 11). The area-specific conductances reported here for the acid and basic zones are also similar to those reported for *Chara* cells suspended in air[4]. There is thus now firm evidence that different regions of the membrane of illuminated cells of *Chara* can be simultaneously in two different "states," even when bathed in an electrolyte solution. It must be stressed that there is probably no "true" value of $G_B$ or $G_A$, but that they will vary from cell to cell and depend in a complicated fashion upon the history of illumination and the cellular environment.

In the basic zones the high conductance appears to be predominantly a consequence of the passive proton (alternatively hydroxyl) uniport proposed by Bisson and Walker (1980, 1981). In the acid zones there appear to be significant contributions to the total conductance from both the passive potassium uniport (e.g. Hope & Walker, 1961; Smith & Walker, 1981) and the electrogenic proton pump (e.g. Spanswick, 1971, 1974*a*, *b*; Richards & Hope, 1974; Keifer & Spanswick, 1978; Smith & Beilby, 1983). The high area-specific conductance of the basic zones is possible if the proton influx occurs through these zones and is predominantly passive (i.e. the contributions of various proton symports and inward electrogenic transport are small). Then in the steady state the proton influx in the basic regions should equal the efflux produced by the proton pump in the acid regions. As the basic zones only cover a small fraction of the membrane area (typically $<20\%$ for the cells reported here), and their membrane PD is expected to be close to their proton equilibrium PD, a high conductance would then be consistent with a high area-specific proton influx.

### *Removal of Illumination*

The conductance of both the acid and basic zones was found to slowly decrease upon removal of the illumination. Eventually, after some hours, the membrane appeared to be reasonably electrically homogeneous. An interesting feature, however, was that although the current flowing between the acid and basic regions disappeared within a few seconds of the removal of illumination, a reasonably high conductance of the basic zones remained for a considerable period (e.g. *see* Fig. 6). A possible explanation is that the basic region can be temporarily maintained in this state by a high local pH maintained by dissociation of the calcium carbonate precipitated in the cell wall. The high con-

[4] *See* footnote 3, p. 193.

ductance is consistent with no flow of current between the acid and basic zones if the membrane PD in the basic zones is then equal to their proton equilibrium PD. The percentage increase in conductance upon illumination varied considerably between the basic (~1800%) and acid (~400%) zones (*see* Table).

*Comparison between $I(x)$ and $V(x)$*

When current is injected into a spatially inhomogeneous cell at a single point, the resultant membrane PD $V(x)$ will decrease monotonically with distance away from the point of current injection. If the dimensions of the various inhomogeneous regions are comparable with their cable lengths, the decay within each region will be primarily determined by its intrinsic cable length (e.g. *see* Fig. 6 of Smith, 1983). The behavior of $I(x)$ is more complicated, however. Because $I(x) = V(x)G(x)$, changes in $G$ at the boundaries between the various regions will also have an effect. Thus the spatial dependence of $I(x)$ will not depend only upon the cable lengths of the regions involved, but also upon the behavior of $G(x)$ in the transitional regions. The situation is further complicated by the finite spatial resolution of the current probe used. This seems to be the explanation for the complicated behavior of $I(x)$ that was sometimes recorded and which made it difficult to resolve $\lambda_A$ and $\lambda_B$. The area-specific conductance can still be estimated in this situation, however, because the important feature is a knowledge of the longitudinal distance over which most of the injected current flows through the membrane. The results obtained by the two independent techniques (i.e. $I(x)$ and $V(x)$) are in good agreement. This suggests that problems were not caused by the insertion of the micropipettes. The results presented have been calculated assuming that the electrical properties were radially symmetric and that abrupt transitions occurred between zones at the boundaries indicated by phenol red. Both assumptions will presumably be a minor source of error.

*Consequences for Electrical Measurements*

The measurements presented in the Table clearly reveal that the area-specific membrane conductance of illuminated *Chara* cells (and also cells only briefly exposed to the dark) is quite different when current is injected into different zones of a cell, and is thus spatially inhomogeneous. This appears to be directly linked to pH banding, the presence of which has been inferred from measurements in this laboratory over a wide range of pH in fast-flowing, strongly buffered bathing solutions (e.g. Smith, Smith, Smith & Walker, 1981). Indeed recent measurements show that this spatial inhomogeneity in conductance is still present when the pH of a solution flowing past the cell is varied from approximately pH 5 to 10. Thus the spatial inhomogeneity in conductance is likely to be present to some extent under most experimental conditions. The main exceptions will be for cells that have been exposed to the dark for some time, and also for extreme values of external pH when pH banding ceases and the cell surface is then at a uniform pH.

As is discussed elsewhere in detail (Smith, 1983), the presence of such inhomogeneities can drastically alter the relationships between the measured conductance and the actual area-specific value at the point of current injection. Generally this will produce a severe underestimation of the calculated area-specific conductance for current injection into the basic zones, and a slight overestimation for acid zones. Thus measurements made without a knowledge of the degree of inhomogeneity present might typically return maximum values of ~0.5 to 0.8 $S/m^2$ (*see* Smith, 1983). However, measurements performed under conditions where a uniform membrane PD is assured (i.e. space-clamping) will yield a correct spatially averaged conductance of all the zones present. Thus in this situation highly conductive, basic regions (if present) will make a proportional contribution to the measured conductance.

If the highly conductive, basic zones reported in this paper are indeed normally present in illuminated *Chara* cells, it would be expected that space-clamped measurements should be on the average significantly higher than those made via point current injection. Figure 10 shows histograms of the membrane conductance measured by these two techniques taken from 37 publications. It is apparent that the area-specific conductances measured via space-clamping are generally higher than those measured by point current injection. The range of values returned by space-clamp techniques was 0.5 to 2.0 $S/m^2$, which is approximately consistent with an admixture of the values reported herein for the individual acid and basic zones. The difference in the histograms may, to some extent, be influenced by the varying numbers of experiments on *Chara* and *Nitella* (i.e. the conductance of *Nitella* is usually less than that of *Chara*). Thus while Fig. 10 is by no means conclusive, it does suggest that previous measurements on *Chara* made via point current injection may have been

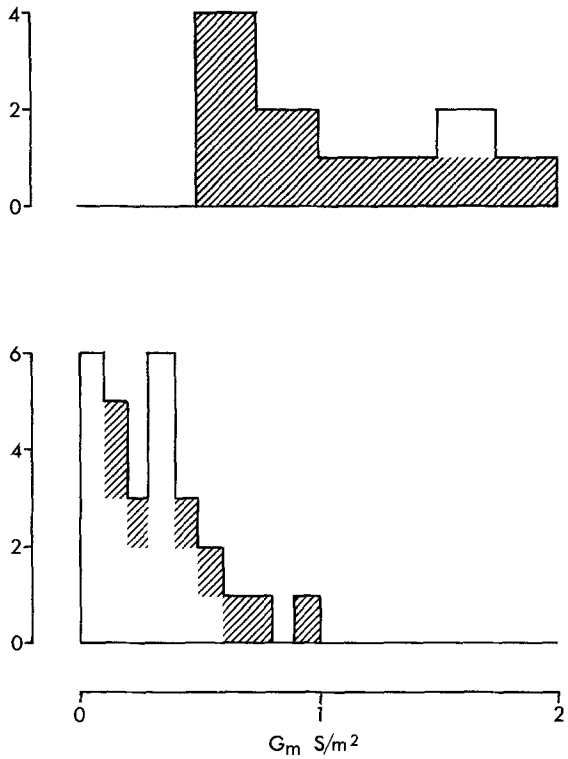


**Fig. 10.** Histograms of the membrane conductances of *Chara* and *Nitella* gleaned from 37 publications available to one of the authors (JRS). Data was only included for experiments where the bathing solution contained ~0.1 mM KCl with pH 5.5 to 6.5. In general the solutions were unbuffered and most publications gave no information on the flow rate used. In the few cases where information upon the degree of illumination was given, the data for cells in bright illumination were included. The upper histogram presents the data from experiments with a geometry that ensured a uniform membrane PD (i.e. space clamping) even if $\lambda_B$ was as small as 2 mm. The lower histogram shows data from experiments where point current injection was used into cell regions of lengths >5 mm. The shaded and clear areas on the histograms refer to results from *Chara* and *Nitella*, respectively

systematically underestimating the true average area-specific membrane conductance.

### *Variations in the Extent of pH Banding*

If the relative areas and properties of the acid and basic zones in a cell membrane vary during an experiment, the measured conductance for the whole cell will vary. The possibility of such variations is supported by measurements on short whorl cells (<3 mm), which are usually unable to maintain a temporally stable, spatially distinct pattern of acid/basic regions. An individual region of these cells can, however, become alternately acid or basic over a period of hours. Measurements made via space-clamping on such cells reveal that the membrane conductance can vary between 0.5 and 4.0 S/m$^2$ over several hours (J.R. Smith, *unpublished*). Such variations in measured conductance would be reduced for measurements made via point current injection, but may in part explain some previously reported long-term conductance variations (e.g. Skierczynska, 1968; Spanswick, 1970, Skierczynska et al., 1972). Thus the decrease in conductance reported after electrode insertion (Spanswick, 1970; Skierczynska et al., 1972) could be partially a consequence of the inhibition of pH banding.

Variations in the extent of pH banding could also be responsible in some degree for the widely varying values of the area-specific membrane conductance reported in the literature (e.g. *see* Fig. 10). The values calculated from measurements would then depend in a complicated fashion upon both the level and history of illumination, and the geometry and nature of the electrodes used.

This work was supported by the Australian Research Grants Committee.

## References

Bell, D.J., Coster, H.G.L., Smith, J.R. 1975. A computer based, four-terminal impedance measuring system for low frequencies. *J. Phys. E* **8**:66–70

Bisson, M.A., Walker, N.A. 1980. The *Chara* plasmalemma at high pH. Electrical measurements show rapid specific passive uniport of $H^+$ or $OH^-$. *J. Membrane Biol.* **56**:1–7

Bisson, M.A., Walker, N.A. 1981. The hyperpolarization of the *Chara* membrane at high pH: Effects of external potassium, internal pH, and DCCD. *J. Exp. Bot.* **32**:951–971

Bisson, M.A., Walker, N.A. 1982. Transitions between modes of behaviour (states) of the charophyte plasmalemma. *In:* Plasmalemma and Tonoplast: Their Functions in the Plant Cell. D. Marme, E. Marre and R. Hertel, editors. pp. 35–40. Elsevier Biomedical Press, Amsterdam

Bradley, J., Williams, E.J. 1967. Chloride electrochemical potentials and membrane resistances in *Nitella translucens*. *J. Exp. Bot.* **18**:241–253

Chilcott, T.C., Coster, H.G.L., Ogata, K., Smith, J.R. 1981. Spatial distribution of the electrical properties and electrogenic pumps in *Chara corallina*. *XIII International Botanical Congress Abstracts*, p. 9

Coster, H.G.L., Smith, J.R. 1977. Low-frequency impedance of *Chara corallina*: Simultaneous measurements of the separate plasmalemma and tonoplast capacitance and conductance. *Aust. J. Plant Physiol.* **4**:667–674

Hogg, J., Williams, E.J., Johnston, R.J. 1969. The membrane electrical parameters of *Nitella translucens*. *J. Theor. Biol.* **24**:317–334

Hope, A.B., Walker, N.A. 1961. Ionic relations of cells of *Chara australis*. IV. Membrane potential differences and resistances. *Aust. J. Biol. Sci.* **14**:26–44

Keifer, D.W., Spanswick, R.M. 1978. Activity of the electrogenic pump in *Chara corallina* as inferred from measurements of the membrane potential, conductance and potassium permeability. *Plant Physiol.* **62**:653–661

Lucas, W.J., Smith, F.A. 1973. The formation of acid and alkaline regions at the surface of *Chara corallina* cells. *J. Exp. Bot.* **24**:1–14

Richards, J.L., Hope, A.B. 1974. The role of protons in determining membrane electrical characteristics in *Chara corallina*. *J. Membrane Biol.* **16**:121–144

Skierczynska, J. 1968. Some of the electrical characteristics of the cell membrane of *Chara australis*. *J. Exp. Bot.* **19**:389–406

Skierczynska, J., Zolnierczuk, R., Spiewla, E., Bulanda, W., Przygodzka, A. 1972. Measurements of membrane resistance of characeae with external electrodes and microelectrodes. *J. Exp. Bot.* **23**:591–599

Smith, F.A., Smith, J.R., Smith, P.T., Walker, N.A. 1981. Bicarbonate assimilation by proton pumping in charophyte plants. *XIII International Botanical Congress Abstracts*, p. 227

Smith, J.R. 1983. Effect of a spatially inhomogeneous membrane upon the measured electrical properties of *Chara*. *J. Membrane Biol.* **73**:185–192

Smith, J.R., Beilby, M.J. 1983. Inhibition of electrogenic transport associated with the action potential in *Chara*. *J. Membrane Biol.* **71**:131–140

Smith, P.T., Walker, N.A. 1981. Studies on the perfused plasmalemma of *Chara corallina*: I. Current-voltage curves, ATP and potassium dependence. *J. Membrane Biol.* **60**:223–236

Spanswick, R.M. 1970. Electrophysiological techniques and the magnitudes of the membrane potentials and resistances of *Nitella translucens*. *J. Exp. Bot.* **21**:617–627

Spanswick, R.M. 1972. Evidence for an electrogenic ion pump in *Nitella translucens*. I. The effects of pH, $K^+$, $Na^+$, light and temperature on the membrane potential and resistance. *Biochim. Biophys. Acta* **288**:73–89

Spanswick, R.M. 1974*a*. Evidence for an electrogenic ion pump in *Nitella translucens*. II. Control of the light-stimulated component of the membrane potential. *Biochim. Biophys. Acta* **332**:387–398

Spanswick, R.M. 1974*b*. Hydrogen ion transport in giant algal cells. *Can. J. Bot.* **52**:1029–1034

Spear, D.J., Barr, J.K., Barr, C.E. 1969. Localisation of hydrogen ion and chloride ion fluxes in *Nitella*. *J. Gen. Physiol.* **54**:397–414

Volkov, G.A., Platonova, L.V. 1970. Electrical properties of the cells of the alga *Nitella flexilis*. I. Cable theory in the conditions of transitional and steady regimes with reference to the finite length of the cell and the resistance of the ends of the cell. *Biofizika* **15**:635–642

Walker, N.A. 1980. The transport systems of charophyte and chlorophyte giant algae and their integration into modes of behaviour. *In*: Plant Membrane Transport: Current Conceptual Issues. R.M. Spanswick, W.J. Lucas and J. Dainty, editors. pp. 287–304. Elsevier/North Holland, Amsterdam

Walker, N.A., Smith, F.A. 1977. Circulating electric currents between acid and alkaline zones associated with $HCO_3^-$ assimilation in *Chara*. *J. Exp. Bot.* **28**:1190–1206

Williams, E., Johnston, R.J., Dainty, J. 1964. The electrical resistance and capacitance of the membranes of *Nitella translucens*. *J. Exp. Bot.* **15**:1–14

Received 28 April 1982; revised 18 October 1982